

Deep Cortical Layers Are Activated Directly by Thalamus

Christine M. Constantinople and Randy M. Bruno*

The thalamocortical (TC) projection to layer 4 (L4) is thought to be the main route by which sensory organs communicate with cortex. Sensory information is believed to then propagate through the cortical column along the L4→L2/3→L5/6 pathway. Here, we show that sensory-evoked responses of L5/6 neurons in rats derive instead from direct TC synapses. Many L5/6 neurons exhibited sensory-evoked postsynaptic potentials with the same latencies as L4. Paired *in vivo* recordings from L5/6 neurons and thalamic neurons revealed substantial convergence of direct TC synapses onto diverse types of infragranular neurons, particularly in L5B. Pharmacological inactivation of L4 had no effect on sensory-evoked synaptic input to L5/6 neurons. L4 is thus not an obligatory distribution hub for cortical activity, and thalamus activates two separate, independent “strata” of cortex in parallel.

The conventional model of neocortex is that sensory processing begins in L4, which has been known for a century to be the principal target of thalamic afferents. Cortical layers are believed to transform sensory information as excitation spreads serially along the L4→L2/3→L5/6 pathway (1–4). This hierarchical serial model is consistent with anatomical observations that axons of excitatory L4 neurons primarily innervate L2/3 and that axons of L2/3 pyramidal neurons arborize extensively in L5/6 (1, 4). L5 neurons make up a major output of the cortex, as they have the most substantial axonal innervation of subcortical and cortical structures, whereas L6 neurons transmit feedback to thalamus and cortex (4–6).

The same thalamocortical (TC) axons that arborize so extensively in L4 also have sparser branches in the infragranular layers at the L5–L6 border (7–11), which have been assumed to be modulatory (3, 11, 12). Recent quantitative measurements of reconstructed TC axons suggest, however, that innervation of L5/6 may be extensive, albeit less than that of L4 (8). Therefore, L5/6 neurons might integrate sensory information from at least two classes of inputs: the direct TC pathway and the indirect L4→L2/3→L5/6 pathway. We investigated this in adult rats administered local anesthetics and a sedative, which better approximate wakefulness than does general anesthesia (13, 14). We made *in vivo* whole-cell recordings from 176 neurons in barrel cortex and juxtosomal recordings from 76 neurons in ventral posterior medial (VPM) nucleus of thalamus, areas processing tactile input from the facial whiskers during environment exploration.

The conventional model predicts that the responses of neurons in L5/6 should lag behind those in other layers. We compared the latencies of sensory-evoked sub- and suprathreshold responses of morphologically identified neurons in every layer of barrel cortex. Strong high-velocity

whisker deflection evoked robust postsynaptic potentials (PSPs) in neurons in all cortical layers (Fig. 1A). L4 onset latencies preceded those in L2/3 (L4: 7.76 ± 0.16 ms, $n = 24$; L2/3: 11.04 ± 0.26 ms, $n = 18$; $P < 10^{-13}$) (Fig. 1, B and C). While the average L5 (9.44 ± 0.3 , $n = 53$) and L6 latencies (10.68 ± 0.67 ms, $n = 13$) were longer than that of L4, many L5 cells rivaled L4 in latency. Moreover, the longer-latency PSPs among L5 cells occur simultaneously with, not after, the onsets of L2/3 cells (Fig. 1, B and C). Many L5 cells exhibited spike latencies as short as cells in L4 (Fig. 1, D to F).

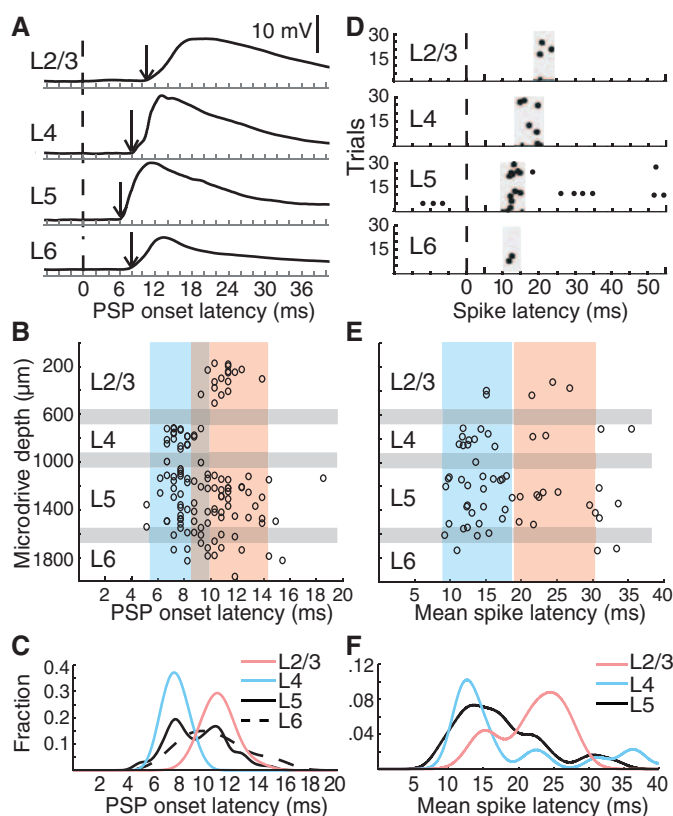
Short L5/6 latencies could result from substantial TC convergence, which can be estimated

from the probability of finding TC–L5/6 connections. Ideally, synaptic measurements are made *in vivo* rather than *in vitro* to avoid issues related to lack of background synaptic input, the concentrations of extracellular ions and neuromodulators, and severing of axons during slice preparation. We used a previously developed technique to identify and quantify individual synaptic connections in living animals (14). Whole-cell recordings were made from neurons in L5/6 during simultaneous juxtosomal recording of action potentials from somatotopically aligned VPM neurons (Fig. 2, A and B). The average PSP (aPSP) that a single thalamic cell produces in a cortical neuron (Fig. 2, C and D) was estimated by spike-triggered averaging and corrected for the contribution of unrecorded inputs [see supplementary materials (SM)].

Monosynaptic connections were observed onto L5/6 neurons (10 of 55 topographically aligned pairs tested, including morphologically identified and unidentified cells). Of the morphologically identified subset (Fig. 2E), connections were observed more frequently onto L5 pyramidal neurons (26%, 7 connected of 27 pairs tested) than onto L6 cells (9%, 1 of 11). Connections were not observed onto topographically unaligned cells or pyramidal neurons with apical trunks extending through the septal region between L4 barrels (Fig. 2E).

Individual TC connections onto infragranular neurons produced relatively small depolarizations (mean \pm SD 571 ± 46.5 μ V, median 463 μ V,

Fig. 1. Many L5/6 cells have response latencies as short as L4's. (A) Example whole-cell traces from histologically identified cells, averaged overall stimulus directions. Dashed line, time of whisker deflection; arrow, PSP onset. (B) PSP onset latencies by microdrive depth ($n = 126$). Gray bars, approximate laminar boundaries determined from the microdrive depths where histologically recovered neurons were found in each layer. Blue and pink boxes, approximate extent of the densities of L4 and L2/3 data, respectively, as in (C). (C) Normalized probability densities of PSP onset latencies. (D) Example raster plots of cells in each layer relative to whisker deflection. (E) Distribution of mean spike latencies for responsive cells ($n = 64$) by microdrive depth. (F) Normalized probability densities of mean spike latencies. L6 density was not calculated because of insufficient spiking.



Department of Neuroscience and Kavli Institute for Brain Science, Columbia University, New York, NY 10032, USA.

*Corresponding author. E-mail: randybruno@columbia.edu

range 137 μ V to 1.18 mV (Fig. 2F), similar to TC-L4 synapses [\sim 500 μ V (14)]. Mean onset latencies and 20 to 80% rise times were 2.40 ± 0.31 and 6.17 ± 4.55 ms, respectively. Neurons in each layer responded to conventional high-velocity stimuli with PSPs proportional to the probability of finding TC connections in that layer (Fig. 2G), consistent with direct TC connections producing sensory-evoked responses.

L5/6 neuronal subclasses having distinct morphology, physiology, and projection targets are spatially intermingled (15, 16) but may be preferentially thalamorecipient (9). Monosynaptic TC connections were observed most frequently on L5 thick-tufted neurons (44%, 4 connected of 9 pairs tested) but were also observed on L5 thin-tufted (17%, 3 of 18) and L6 (9%, 1 of 11) pyramidal neurons (Fig. 2, H and I, and fig. S1A) and smooth interneurons (1 of 3). In vitro L5 thick-tufted neurons are typically “intrinsically bursting” (IB), whereas adapting trains of single spikes are more typical of the “regular-spiking” (RS) L5 thin-tufted neurons (9, 16). The predominant firing type of both morphological classes in vivo, however, was IB (fig. S1, B and C), possibly because of our awakelike conditions, and monosynaptic connections were observed onto

both physiological cell types (fig. S1, D and E). By contrast, most connected cells had somata at depths of 1400 to 1600 μ m, where thalamic axons arborize in L5B/6A (7, 8), even though we sampled substantially from depths shallower than 1400 μ m (Fig. 2J, left). Neurons in the TC arborization zone near L5B had the largest sensory-evoked PSPs (Fig. 2J, right).

Given that a whisker’s representation in VPM contains \sim 200 neurons (14), 9 to 44% convergence is substantial, translating into \sim 20 to 90 thalamic connections per L5/6 cell, depending on its type. Although individual TC synapses are weak, this number of synchronous convergent inputs may provide a second powerful pathway into the cortex, capable of directly driving the activity of L5 and responsive L6 cells. We therefore sought to dissect the contributions of the direct TC pathway and the indirect L4 \rightarrow L2/3 \rightarrow L5/6 pathway to the sensory responses of infragranular neurons, by inactivating L4 during sensory stimulation. Silencing of L4 was achieved by pressure ejection of lidocaine and confirmed by monitoring the local field potential (LFP) through the drug pipette. Beyond blocking action potentials in L4 cells, lidocaine suppresses axonal conduction within L4, along

TC axonal branches that extend directly into L3, and along the radial trunks of axons from L2/3 cells that traverse L4 to synapse in L5/6. This manipulation thus disconnects the upper and lower cortical layers, leaving intact the TC-L5/6 pathway.

To validate our manipulation, we performed whole-cell recordings of L4 neurons located 150 μ m from the LFP and drug pipette (Fig. 3A). Lidocaine injection not only prevented these L4 cells on the other side of the barrel from discharging any action potentials but also robustly and reliably eliminated virtually all spontaneous and sensory-evoked synaptic input ($n = 6$, from 10.71 ± 1.21 to 0.27 ± 0.08 mV, $P = 0.0004$) (Fig. 3, B to D). Given the high connectivity among L4 barrel neurons [$P(\text{connection}) \sim 0.3$ (4)], this dramatic reduction in synaptic input confirms that our manipulation silenced virtually all neurons in a barrel. Replacing the whole-cell pipette with an LFP pipette yielded similar results (fig. S2, A to C), which further demonstrated that lidocaine inactivated a diameter exceeding 300 μ m, more than the size of a barrel (\sim 200 to 300 μ m wide). In addition, L4 inactivation reduced L2/3 synaptic inputs and prevented L2/3 spiking (fig. S2, D to F).

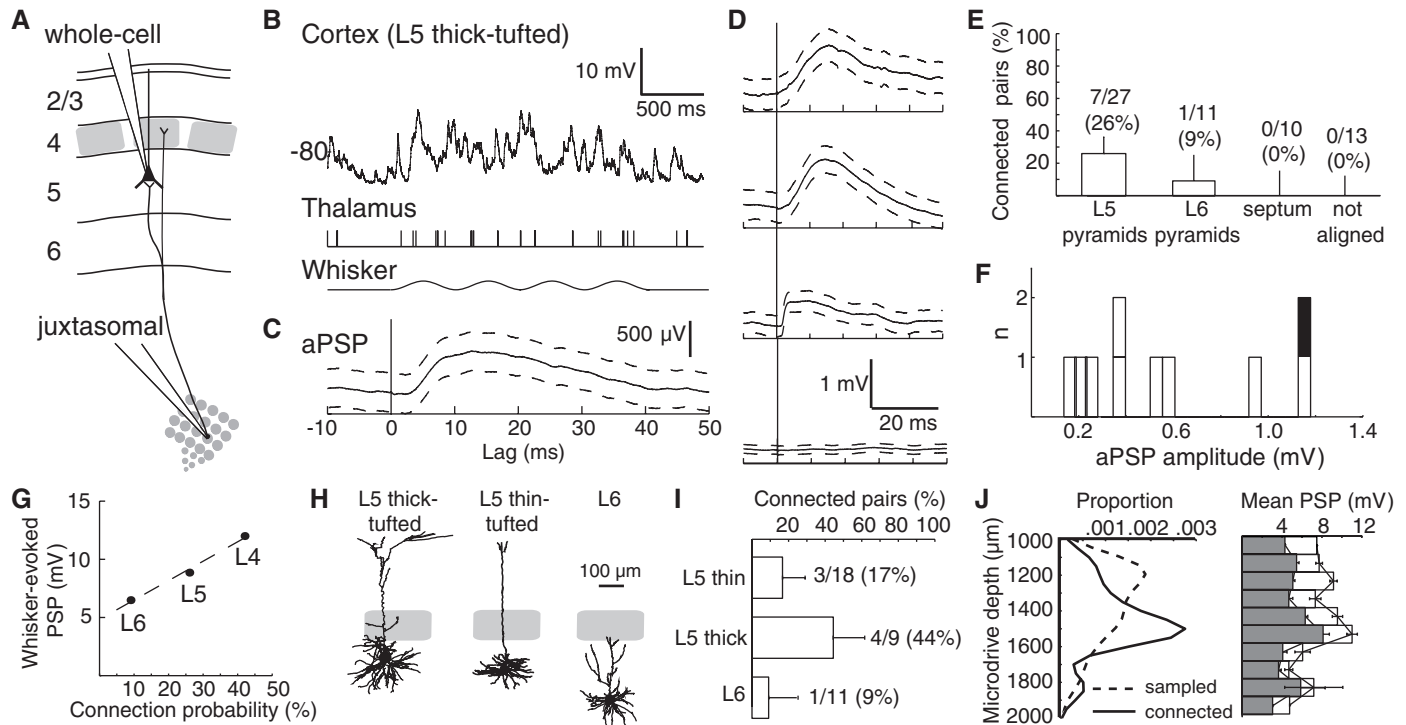


Fig. 2. TC connections onto infragranular neurons are weak but convergent. (A) Schematic of simultaneous in vivo whole-cell recording of a cortical L5 pyramidal neuron and juxtosomal recording of a somatotopically aligned thalamic neuron. (B) Example whole-cell trace from an L5 thick-tufted cell (top), action potentials from a thalamic neuron (middle), and sinusoidal whisker stimulus (bottom). (C) The aPSP measured from the above pair ($n = 1076$ thalamic action potentials). Dashed lines, 95% confidence intervals. (D) Example aPSPs onto L5 thin-tufted, L6, and L5 thick-tufted pyramidal neurons and example unconnected pair (from top to bottom). (E) Percentage of connected pairs by cortical cell location. Error bars, 95% confidence intervals

for a binomial distribution. (F) Distribution of aPSP amplitudes. Black, smooth interneuron. (G) Amplitude of mean sensory-evoked PSPs (10 to 20 deflections in the preferred direction) for L4, L5, and L6 cells ($n = 40, 35$, and 11 , respectively) versus probability of finding connected pairs in each layer. Dashed line, least-squares fit. L4 data are from (14). (H) Example reconstructions. (I) Connection probability by morphological subtype. (J) (Left) Densities of the depths of all sampled cells (dashed line) and cells onto which TC connections were observed (solid line). (Right) Mean sensory-evoked PSP amplitude by depth (means \pm SEM; 100- μ m bins). White bars, preferred direction. Shaded bars, average over eight directions.

We then recorded synaptic inputs from morphologically identified neurons in L5/6 while inactivating the overlying L4 barrel (Fig. 3E). L5/6 pyramidal neurons deeper than 1350 μm from the pia were targeted to avoid direct drug effects on recorded cells and to sample the region of highest TC connectivity (Fig. 2J). Despite reducing the amplitude of the sensory-evoked LFP in L4 ($n = 12$; from 0.69 ± 0.09 to 0.21 ± 0.03 mV, $P = 0.0001$), lidocaine had virtually no effect on the sensory-evoked synaptic inputs of L5/6 neurons (Fig. 3, F and G), in terms of amplitude (from 7.53 ± 0.98 to 7.58 ± 0.75 mV, $P = 0.93$) (Fig. 3H) or onset latency (fig. S3, A and B). Mean and variance of spontaneous membrane potential fluctuations were similarly unaffected (fig. S3B).

Even after L4 inactivation, sensory stimuli continued to evoke L5/6 action potentials (0.16 ± 0.07 versus 0.12 ± 0.04 spikes per stimulus, $P = 0.64$) (Fig. 3, I and J). Although L5/6 spiking was unaffected on average, some individual neurons appeared to increase or decrease their firing rates (Fig. 3J). To test whether this was simply because of spiking variability, L5/6 spiking re-

sponses during “test” and subsequent “retest” periods were compared. Individual L5/6 cells exhibited a range of firing rate differences between the test and retest periods similar to the pre- and postlidocaine periods (fig. S3C).

How can thalamus effectively elicit L5 spikes given that L5 receives less TC convergence and exhibits smaller PSPs than L4? The mean spontaneous membrane potential of each L5 neuron was significantly closer to its spike threshold, compared with neurons in L4 and L6 (Fig. 3K), and the distance to threshold correlated with responsiveness (fig. S3E). Therefore, the relative depolarization of L5 cells observed here under sedation, as under anesthesia (17), enables less synaptic input than available to L4 to become suprathreshold in 53% of cells (fig. S3, F and G). In contrast, the smaller sensory-evoked PSPs and relative hyperpolarization of L6 (Figs. 2G and 3K) render 81% of its cells silent (fig. S3, F and G), consistent with L6 corticothalamic cells being unresponsive to sensory stimulation [see (6)].

Muscimol injection to inactivate VPM neurons but spare fibers of passage substantially re-

duced PSPs of aligned L5/6 neurons (fig. S4, A and B). Residual PSP did not derive from neighboring cortical columns (fig. S4, C and D). A likely source is the secondary thalamic area, the posterior medial (POM) nucleus, which arborizes in L1 and L5A, consistent with some L5 cells receiving mixed VPM and POM input (18). We tested whether long-range inputs—including axons from POM, secondary somatosensory cortex, primary motor cortex, and the callosum—contribute to L5 sensory responses via synapses onto apical tufts in L1. Pial application of lidocaine blocks L1 synapses, as indicated by its ability to silence L2 (fig. S5, A to C). L5 PSPs were unaffected by combined L1/L4 inactivation (fig. S5, D and E). If ascending pathways such as those from POM contribute to deep-layer sensory responses, it is likely that they do so via axon collaterals in L5/6 rather than in L1.

Our study demonstrates that primary thalamic nuclei, like VPM, can simultaneously copy the same signals to L4 and L5B, where they are processed in parallel (Fig. 4B) instead of serially through L4 (Fig. 4A). The TC→L4→L2/3

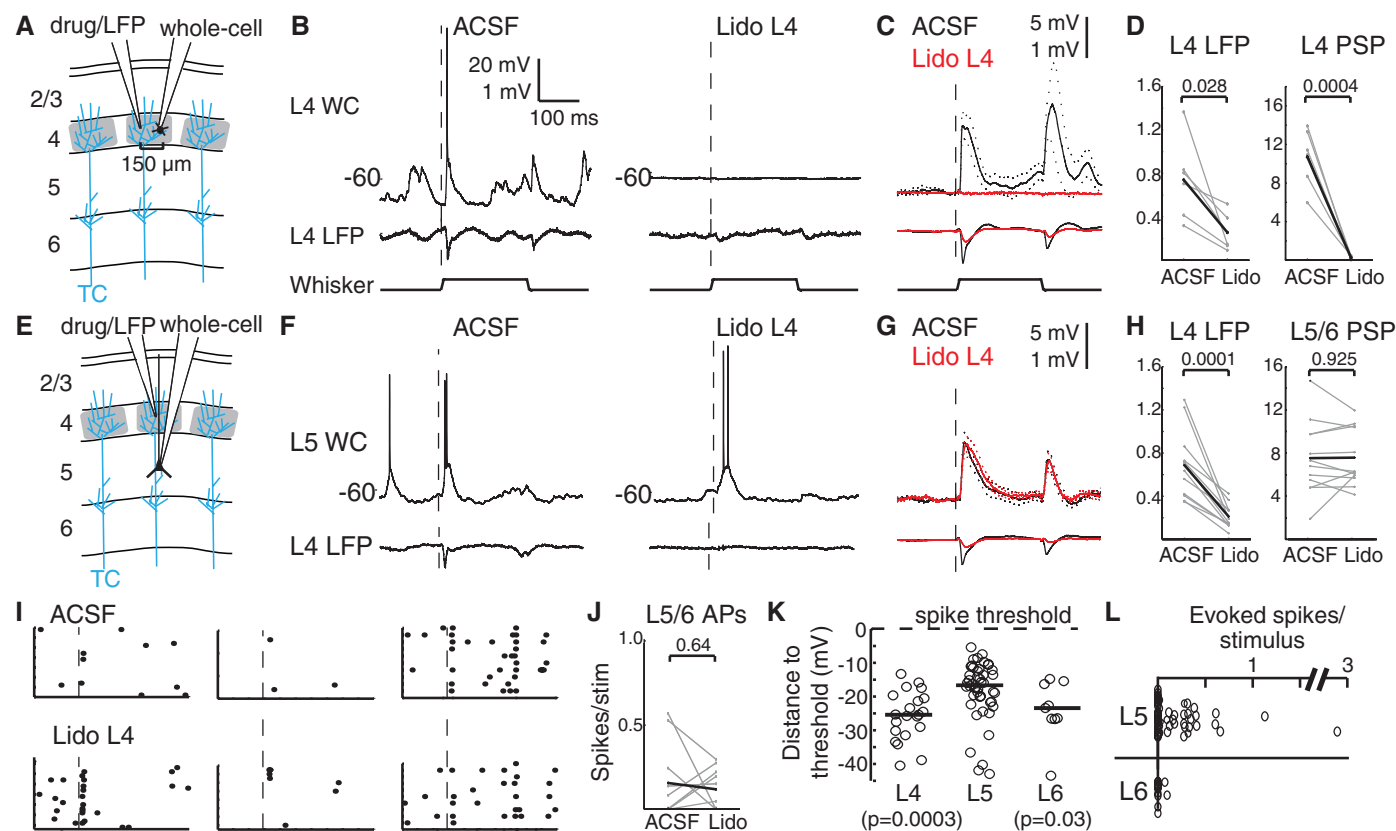


Fig. 3. L5/6 sensory responses do not require L4. (A) Whole-cell recordings were made from L4 cells during inactivation of the barrel by lidocaine injection. Blue lines schematically depict single TC axons, among hundreds per column. (B) Simultaneous whole-cell and LFP recordings during injection of artificial cerebrospinal fluid (ACSF) vehicle and lidocaine. Dashed line, onset of whisker deflection in preferred direction. (C) Population averages of L4 PSPs (top) and LFPs (bottom). Dotted lines, SEM. (D) Summary of responses (in mV). Gray, individual cells; black, means. (E) L5/6 recordings were made while L4 was silenced. (F) Example L5 whole-cell and L4 LFP traces

during injection of ACSF and lidocaine. (G) Population averages of L5/6 PSPs (top) and L4 LFPs (bottom). (H) Summary plots. (I) Rasters of a subset of trials for three example neurons during injection of ACSF (top) and lidocaine (bottom). (J) Plots of the baseline-subtracted evoked spikes per stimulus before and after lidocaine injection. (K) The relation between neurons' mean spontaneous membrane potential and spike threshold (L4: $n = 21$; L5: $n = 46$; L6: $n = 9$). Circles, individual cells; lines, medians; P values, comparison with L5 (Wilcoxon rank-sum test). (L) Baseline-subtracted evoked spikes per stimulus.

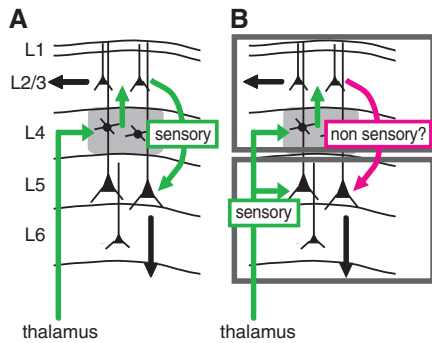


Fig. 4. Schematics of the conventional and proposed models of cortical processing. (A) In the conventional serial model, sensory information is transformed as excitation spreads from thalamus to L4 to L2/3 to L5/6 along the densest axonal pathways (green). (B) In the bistratified model, thalamus copies sensory information to both an upper stratum (L4 and L2/3) and a lower stratum (L5/6), which differ in coding properties and downstream targets.

pathway and the TC→L5/6 pathway appear independent with regard to ascending sensory signals. TC axons innervate both middle and deep layers in multiple species (human, monkey, rat, and cat) and neocortical systems (motor, visual, auditory, and somatosensory) (19–23). Tuning of extracellular units in infragranular layers of cat visual and rodent somatosensory cortex often persists following lesion of L2/3 (24, 25), and some such units respond as early as middle layers (26, 27). Direct TC engagement of infragranular neurons may therefore be a general feature of neocortex.

Neocortical columns may contain two separate processing systems or “strata”: an upper stratum (L4 and L2/3) and a lower stratum (L5/6) possibly subserving different functions. This architecture may elaborate receptive fields via intralaminar cross-columnar rather than in-

terlaminar connections. Moreover, L2/3 targets other neocortical regions, whereas L5/6 targets both cortical and subcortical structures. Although some subcortical projections provide feedback (i.e., to brainstem and primary thalamic nuclei), many of the subcortical targets, especially those of L5, are action-related (striatum and spinal cord) or high-order (secondary thalamic nuclei, which innervate high-order cortical regions). Both strata therefore have direct access to the same sensory information and can alter behavior via different anatomical pathways. Consistent with the idea of two distinct systems, cell fate mapping studies recently demonstrated that the upper and lower strata develop from two distinct populations of radial glial cells (28).

Our results further demonstrate that propagation of excitation cannot be inferred solely from synaptic strength or relative axonal densities. L2/3's extremely low firing rates (13, 29–31) may explain its minimal contribution to sensory signals in deep layers, which, by contrast, are highly active. The activity and interactions of the layers may be behaviorally gated by comparisons of motor, state, and sensory signals (6, 32, 33) or by induction of learning.

References and Notes

1. C. D. Gilbert, T. N. Wiesel, *Nature* **280**, 120 (1979).
2. R. J. Douglas, K. A. Martin, *Annu. Rev. Neurosci.* **27**, 419 (2004).
3. E. M. Callaway, *Neural Netw.* **17**, 625 (2004).
4. D. Feldmeyer, *Frontiers Neuroanat* **6**, 24 (2012).
5. M. Oberlaender *et al.*, *Proc. Natl. Acad. Sci. U.S.A.* **108**, 4188 (2011).
6. S. Lee, G. E. Carvell, D. J. Simons, *Nat. Neurosci.* **11**, 1430 (2008).
7. V. C. Wimmer, R. M. Bruno, C. P. de Kock, T. Kuner, B. Sakmann, *Cereb. Cortex* **20**, 2265 (2010).
8. M. Oberlaender, A. Ramirez, R. M. Bruno, *Neuron* **74**, 648 (2012).
9. A. Agmon, B. W. Connors, *J. Neurosci.* **12**, 319 (1992).
10. M. Beierlein, B. W. Connors, *J. Neurophysiol.* **88**, 1924 (2002).
11. A. N. Viae, I. Petrof, S. M. Sherman, *J. Neurosci.* **31**, 12738 (2011).
12. R. W. Guillery, S. M. Sherman, *Neuron* **33**, 163 (2002).

13. C. M. Constantinople, R. M. Bruno, *Neuron* **69**, 1061 (2011).
14. R. M. Bruno, B. Sakmann, *Science* **312**, 1622 (2006).
15. Y. Chagnac-Amitai, H. J. Luhmann, D. A. Prince, *J. Comp. Neurol.* **296**, 598 (1990).
16. A. M. Hattox, S. B. Nelson, *J. Neurophysiol.* **98**, 3330 (2007).
17. I. D. Manns, B. Sakmann, M. Brecht, *J. Physiol.* **556**, 601 (2004).
18. I. Bureau, F. von Saint Paul, K. Svoboda, *PLoS Biol.* **4**, e382 (2006).
19. D. Ferster, S. LeVay, *J. Comp. Neurol.* **182**, 923 (1978).
20. G. G. Blasdel, J. S. Lund, *J. Neurosci.* **3**, 1389 (1983).
21. M. Herkenham, *Science* **207**, 532 (1980).
22. C. L. Huang, J. A. Winer, *J. Comp. Neurol.* **427**, 302 (2000).
23. V. Garcia-Marin, T. H. Ahmed, Y. C. Afzal, M. J. Hawken, *J. Comp. Neurol.* **521**, 130 (2013).
24. H. D. Schwark, J. G. Malpeli, T. G. Weyand, C. Lee, *J. Neurophysiol.* **56**, 1074 (1986).
25. W. Huang, M. Armstrong-James, V. Rema, M. E. Diamond, F. F. Ebner, *J. Neurophysiol.* **80**, 3261 (1998).
26. C. P. de Kock, R. M. Bruno, H. Spors, B. Sakmann, *J. Physiol.* **581**, 139 (2007).
27. J. H. Maunsell, J. R. Gibson, *J. Neurophysiol.* **68**, 1332 (1992).
28. S. J. Franco *et al.*, *Science* **337**, 746 (2012).
29. D. H. O'Connor, S. P. Peron, D. Huber, K. Svoboda, *Neuron* **67**, 1048 (2010).
30. T. Hromádka, M. R. Deweese, A. M. Zador, *PLoS Biol.* **6**, e16 (2008).
31. C. P. de Kock, B. Sakmann, *Proc. Natl. Acad. Sci. U.S.A.* **106**, 16446 (2009).
32. C. M. Niell, M. P. Stryker, *Neuron* **65**, 472 (2010).
33. G. B. Keller, T. Bonhoeffer, M. Hübener, *Neuron* **74**, 809 (2012).

Acknowledgments: We thank L. Abbott, R. Axel, A. Losonczy, and K. Miller for manuscript comments; D. Baughman for technical support; and M. Ilardi for morphological reconstruction. Supported by National Institute of Neurological Disorders and Stroke, NIH, NS069679; Rita Allen Foundation; Klingenstein Fund; and an NSF Student Fellowship.

Supplementary Materials

www.sciencemag.org/cgi/content/full/340/6140/1591/DC1
Materials and Methods
Figs. S1 to S5
References (34, 35)

11 February 2013; accepted 26 April 2013
10.1126/science.1236425